Permeability prediction of soils including degree of compaction and microstructure

Harifidy Ranaivomanana, Andry Razakamanantsoa, Ouali Amiri

Permeability Prediction of Soils Including Degree of Compaction and Microstructure

Harifidy Ranaivomanana, Ph.D.[1]; Andry Razakamanantsoa, Ph.D.[2]; and Ouali Amiri, Ph.D.[3]

Abstract: The present paper deals with the proposition of an original analytical permeability model of compacted soils. The model involves the microstructure of the material through the porosity and the pore-size distribution obtained by mercury intrusion porosimetry (MIP), as well as the degree of compaction. Their effects on the morphological parameters of the porous network (tortuosity and interconnection of pore net-work) are studied. The model was developed and tested on various types of soil: a loamy sand, a gravelous sand, a clay, and an alterite. Samples were compacted with various degrees of compaction: 85, 95, 100, and 105% of the optimum dry density as determined by a standard compac-tion method. The experimental results obtained for both loamy and gravelous sands and for clay were well reproduced by the model, except for the alterite. Such results might be explained by the high brittleness of the alterite, leading to a crumbling phenomenon rather than to its densifica-tion during the compaction process.

Keywords: Permeability; Compacted soils; Microstructure; Modeling; Mercury intrusion porosimetry.

State of the Art

The permeability of a soil is its ability to allow water flow under a hydraulic head. It is one of the most important geotechnical properties of soils and is involved, among other things, in the design of retaining structures and earthen dams. Until now, permeability has not yet been classified as a parameter for design because of several constraints related to its measurement (Shackelford et al. 2000; Aldeef and Rayhani 2014). Permeability measurement is tough, time-consuming, and expensive. Therefore, modeling flows in saturated or unsaturated soils has become common practice in geotechnical engineering. Many analytical equations are often used in the literature to predict the permeability of fine-grained soil, as presented in the following section. However, one of the weaknesses of such approaches remains the insufficient consideration of compaction characteristics. Based on existing models, the main objective and the originality of the present paper is the proposition of a relevant and simple analytical approach of soil permeability determination with particular attention paid to the influence of compaction characteristics and microstructure. For this purpose, the first section addresses a more comprehensive state of the art in the analytical modeling of soil permeability to understand not only the basic principles of the models but also their limitations. The different models presented here are grouped into three categories: (1) models involving microstructural properties of soils, (2) models involving the physical properties and/or granulometric characteristics of soils, and (3) models developed for consolidated materials (rock, concrete) but potentially applicable to soils.

Models Involving Microstructural Properties of Soils

The porous structure of soils can be classified into two parts according to pore sizes: small pores (∼1–200 nm) located within aggregates and associated with textural porosity, and large pores (∼0.2–30 μm) located between aggregates and associated with structural porosity. As reported by Beven and Germann (1982), water flow in soils occurs mainly in macropores. Thus, a description of the latter, generally based on capillary models, has often been proposed in the literature to estimate the soil permeability. Principles and limitations of such capillary models are discussed in the following paragraph.

Straight Capillary Models

For this model, the porous medium is made up of straight parallel channels with a cylindrical shape. The permeability (k) is expressed as a linear function of the porosity and a quadratic function of the characteristic size of the channels

$$k = \frac{pd^2}{32} \tag{1}$$

where p = porosity; and d = mean diameter of channels estimated from the pore-size distribution.

Such an approach is obviously unsatisfactory because it considers only one-dimensional flow and assumes that all pores are involved in the water-flow process. Furthermore, the representation of the porous medium by means of channels with the same size is unrealistic. Finally, the influences of morphological parameters are not taken into account. Thus, by introducing the tortuosity (τ) to

[1]Jr. Researcher, L'Université Nantes Angers Le Mans, Institut de Recherche en Génie Civil et Mécanique (GeM), Unité Mixte de Recherche-Centre National de la Recherche Scientifique 6183, Université de Nantes (Institut Universitaire de Technologie de Saint-Nazaire), 58, Rue Michel Ange, 44606 Saint-Nazaire, France (corresponding author). E-mail: harifidy.ranaivomanana@univ-nantes.fr

[2]Jr. Researcher, Institut Français des Sciences et des Technologies des Transports, de l'Aménagement et des Réseaux (IFSTTAR), L'Université Nantes Angers Le Mans, CS 4 Route de Bouaye, 44344 Bouguenais Cedex, France. E-mail: andry.razakamanantsoa@ifsttar.fr

[3]Full Professor, L'Université Nantes Angers Le Mans, Institut de Recherche en Génie Civil et Mécanique (GeM), Unité Mixte de Recherche-Centre National de la Recherche Scientifique 6183, Université de Nantes (Institut Universitaire de Technologie de Saint-Nazaire), 58, Rue Michel Ange, 44606 Saint-Nazaire, France. E-mail: ouali.amiri@univ-nantes.fr

correct the approximation of straight channels, and by assuming that the channels are oriented in the three directions of space, the porous medium is considered to be isotropic and homogeneous. According to Saffman (1959), Eq. (1) becomes

$$k = \frac{pd^2}{96\tau^2} \tag{2}$$

If the pore-size distribution is known, Eq. (2) becomes

$$k = \frac{p}{96\tau^2}\int \rho^2 f(\rho) d\rho \tag{3}$$

where ρ = pore diameter.

Despite the fact that the expression of the permeability given by Eq. (3) seems to achieve more compared to Eq. (1), it remains unsatisfactory because the tortuosity factor is difficult to estimate experimentally. Furthermore, the interconnection of pores is not considered in the model.

Carman-Kozeny Model

The porous medium is assumed to be made up of tortuous cylindrical channels. However, in such an approach, the permeability is expressed as a function of the specific surface area (A_s) rather than as a function of the characteristic size of the pores. The permeability is provided by the following relationship:

$$k = \frac{p^3}{\kappa A_s^2 \tau^2} \tag{4}$$

where κ = shape factor estimated from the assumptions of the porous network model.

In the geotechnical literature, the Carman-Kozeny equation is often recognized to be valid for granular soils only and not for clay (Taylor 1948; Lambe and Whitman 1969). However, according to Chapuis and Aubertin (2003), such consideration is based on a partial demonstration related to practical reasons (imprecise value of the specific surface, unsteady-state flow, samples not fully saturated) or theoretical reasons (anisotropic permeability). Chapuis and Aubertin (2003) experimentally highlighted that the Carman-Kozeny permeability model is generally valid for most soils.

Serial Type Models

Pore Structure Model Involving Two Pore Sizes

In such a model, the porous medium is composed of identical elementary cells that contain two contiguous coaxial channels of two different sizes. By denoting the diameter of the larger channel as d and that of the smaller one as d' ($d' = \alpha d$, $\alpha < 1$), the permeability can be written as follows:

$$k = \frac{pd^2}{8}\frac{\alpha^4}{(1+\alpha^4)(1+\alpha^2)} \tag{5}$$

For $\alpha = 1$, Eq. (1) is recovered (parallel capillary pores), and for $\alpha = 0$ (clogged channels), the permeability is null. However, even if constrictivity effects are considered in the model, the entire pore-size distribution seems to be more relevant to describe the porosity rather than using two pore sizes only. Such an approach could also be improved by taking tortuosity effects into account and by orienting the channels in the three directions of space.

Pore Structure Models Based on Pore-Size Distribution

The main advantage of such models is the consideration of the entire pore-size distribution to describe the porous medium. The interconnection of the porous network is described by a statistical approach involving the pore-size distribution function (Childs and Collis-George 1950; Garcia-Bengochea 1978). Such models are generally based on simplifying assumptions (tortuosity effects not considered, participation of all pores in water-flow process, unidirectional flow) and require a calibration parameter to reproduce the experimental results. To overcome such a calibration parameter, Juang and Holtz (1986) introduced an empirical function of tortuosity in the function representing the interconnection of the porous network. However, according to Lapierre et al. (1990), water flow through soil is controlled by many parameters other than those provided by the mercury intrusion porosimetry (MIP; mineralogy, water salinity); therefore, soil permeability cannot be estimated from indirect tests.

Models Involving Physical Properties and/or Granulometric Characteristics of Soils

These are models involving parameters related to the grain-size distribution [coefficient of uniformity (C_u), coefficient of curvature (C_c), grain dimension (d_i)] or related to physical properties, such as the Atterberg limits (w_L, w_P, I_p), porosity (n), and void ratio (e) (Table 1). The consideration of the compaction characteristics in such approaches has been proposed by some authors. Wang and Huang (1984) established regression equations for predicting maximum dry density, optimum water content, and permeability for two levels of compaction degree: 90 and 95%. Another method based on evolutionary polynomial regression for prediction of permeability, maximum dry density, and optimum moisture content as functions of some physical properties of soil was developed by Ahangar-Asr et al. 2011). The main disadvantage of those approaches remains their empirical character, limiting their validity to sandy soils for models involving parameters related to grain-size distribution and to plastic soils for models involving the Atterberg limits.

Models Developed for Consolidated Materials but Potentially Applicable to Soils

Such models are based on a description of the pore space by considering the pore-size distribution, the geometry of pores, and their interconnection. Three approaches that are tested later in the present study are presented here: a model developed by Aït-Mokhtar et al. (1999), another one developed by Amiri et al. (2005), and the well-known Katz and Thompson model (Katz and Thompson 1986).

Model Developed by Aït-Mokhtar et al. (1999)

The model developed by Aït-Mokhtar et al. (1999) provides a relationship between permeability and microstructure of consolidated materials. It is based on MIP results associated with an idealized pore-size distribution (polymodal distribution) modeled by a log-normal distribution. The model assumes that the microstructure is made up of parallel and cylindrical pores of equal length but with different radii, surrounded by the volume of the material with a

Table 1. Some Soil Permeability Models Involving Physical Properties

References	Permeability model
Hazen (1892)	$k = C_H d_{10}^2$
Slichter (1898)	$k = \frac{g}{\kappa} \times n^{3.287} \times d_{10}^2$
Kenney et al. (1984)	$k = (0.05 \sim 1) \times d_5^2$
Chapuis (2004)	$k = 1.5 \times \frac{e^3}{1+e} \times \frac{1+e_{\max}}{e_{\max}^3} \times d_{10}^2$

representative unit area of surface. For a polymodal porosity with N pore sizes, the permeability is given by

$$k = \sum_{j=1}^{N} e^{6\xi_j^2} \frac{p_j r_{pmj}^2}{8} \quad (6)$$

where p_j = partial porosity related to a mode of the idealized pore-size distribution; ξ_j = dimensionless location parameter; and r_{pmj} = modified value of a porous mode by considering the location parameter. Despite the fact that the model is easy to use, it assumes the contribution of all pores to the water-flow process (unidirectional flow) and neglects the influence of the morphological parameters associated with the pore structure.

Model Developed by Amiri et al. (2005)

Amiri et al. (2005) proposed an original three-dimensional pore network model from MIP results (polymodal pore-size distribution) to predict the water permeability of cement-based materials by taking tortuosity and constrictivity effects into account (serial-type model).

According to the principles and assumptions on which the model is based, the expression of the permeability is given by

$$k = \frac{\delta p}{24\tau^2} r_n^2 \quad (7)$$

where p = porosity of the material; δ and τ = constrictivity and tortuosity factors, respectively; and r_n = smallest pore size constituting a percolation path, obtained from MIP. The main disadvantage of this model is the empirical estimation of τ due to the lack of experimental techniques for its measurement.

Model Developed by Katz and Thompson (1986)

Other types of models based on the percolation theory have also been developed. One of the most used is the Katz and Thompson model, which provides a relationship between the permeability, critical pore diameter (d_c; diameter at which a path appears connected in the network) determined from MIP, and the formation resistivity factor (σ/σ_0) estimated from conductivity measurements

$$k = \frac{1}{226} d_c^2 \frac{\sigma}{\sigma_0} \quad (8)$$

The limitation of the Katz and Thompson model is the use of a constant (1/226) that varies according to the shape of the pores (Banavar and Johnson 1987; Le Doussal 1989). In contrast, the ratio formation resistivity factor (σ/σ_0) is generally estimated from theoretical considerations due to the complexity of an experimental measurement.

This review of literature allows the discussion of some analytical models that can be used to predict the permeability of soils. Models involving particle-size characteristics and physical properties have been established on the basis of empirical considerations and are valid for some types of soils only. Models based on microstructural parameters are well-founded from a physical point of view. They involve the characteristic parameters of the porous structure: the total porosity, the characteristic pore sizes, and the morphological parameters (tortuosity and interconnection of pores), which are difficult to measure experimentally. Another disadvantage of such models is that the influence of compaction characteristics on permeability is not considered. Thus, the present paper focuses on a relevant prediction of hydraulic conductivity (permeability) of a compacted soil, which takes into account both microstructure and compaction characteristics as well as the granulometric properties (particle shape and grain size) of the soil. Indeed, the compaction process leads to a grain rearrangement that affects the water-flow process by modifying the morphological parameters as confirmed by light microscopy observations (the "Light Microscopic Observation Results" section).

The nature of the tested soils, their physical properties, and their characterization after compaction (from a microstructural and hydraulic point of view) are described in details in the next section. Results of characterization tests are analyzed afterward to understand and to model the link between the evolution of the microstructure and that of the hydraulic conductivity depending on the compaction characteristics.

Materials and Methods

Soils Tested

Four types of soil were used in this study: a silty sand (SS), a gravelous sand (GS), a clay (C), and an alterite (A). These soils come from the northwest of France and were sampled from the current high-speed railway "LGV Bretagne-Pays de la Loire" extension project, which requires a geotechnical investigation of soils encountered on site.

Characterization of Soils before Compaction

Some physical properties of the tested soils are recorded in Table 2. The percentage of elements smaller than 2 μm obtained for all samples shows that they contain silt and clay. Such a result is confirmed by the methylene blue value (MBV) value (MBV < 1.50) and by the plasticity index (I_p) value, which correspond to a plastic soil. The physical properties provided in Table 2 are completed by the grain-size distribution curves obtained from laser granulometry (Fig. 1).

Characterization of Soils after Compaction

The implemented rules of earthworks recommend the use of parameters corresponding to the optimum Proctor. However, these parameters are often difficult to reach in situ. If the water content is relatively manageable and measurable, the influence of the density on earthworks at rest after a cyclic stress is a poorly studied aspect. Thus, the compaction characteristics were chosen in such a way as to follow the evolution of mechanical performances with the same initial water content, corresponding to optimum Proctor normal (OPN). The compaction densities adopted in this study are 85, 95, 100, and 105% of the OPN. The Proctor compaction curves are shown in Fig. 2, and the compaction parameters (dry density and water content) at OPN are summarized in Table 3.

MIP

MIP is the most commonly used method for characterizing the microstructure with the pore-size distribution of porous materials. The technique consists of injecting mercury into a dried and degassed material. To maintain the microstructure, samples were

Table 2. Physical Properties of Soils Tested before Compaction

Nature of soil	% 80 μ	% 2 μ	MBV	w_L	I_p	Specific weight (kN/m^3)
SS	30.00	21.00	1.40	40.00	21.00	27.20
GS	20.00	20.00	1.20	—	—	28.80
C	45.00	32.00	2.87	41.30	17.40	28.80
A	35.00	11.00	0.76	41.10	19.00	27.30

dried by sublimation after a 24-h freezing process. The volume of mercury injected corresponds to the cumulative pore volume accessible to mercury. Assuming that the pores are cylindrical, the relationship between the access diameter (d_c) of the pores and the mercury injection pressure (P) is given by Washburn's law

$$P = -\frac{4\sigma_{Hg}\cos\theta_{Hg}}{d_c} \tag{9}$$

where σ_{Hg} = surface tension of mercury (σ_{Hg} = 0.485 N/m at 25°C); and θ_{Hg} = contact angle of the meniscus solid/mercury (θ = 130° > 90° because mercury is a nonwetting fluid).

The main disadvantage of MIP is the well-known *ink bottle* effect. Indeed, according to the Washburn's law, the larger pores are filled with mercury at low pressures. However, all of those large pores are not directly connected with the surface of the material and are accessible only via smaller pores. Thus, MIP overestimates the volume of small pores and hence underestimates that of the large pores. The MIP tests were carried out on a Micromeritics (Norcross, Georgia) AutoPore IV porosimeter, which is able to characterize pores between 0.06 and 350 μm in diameter.

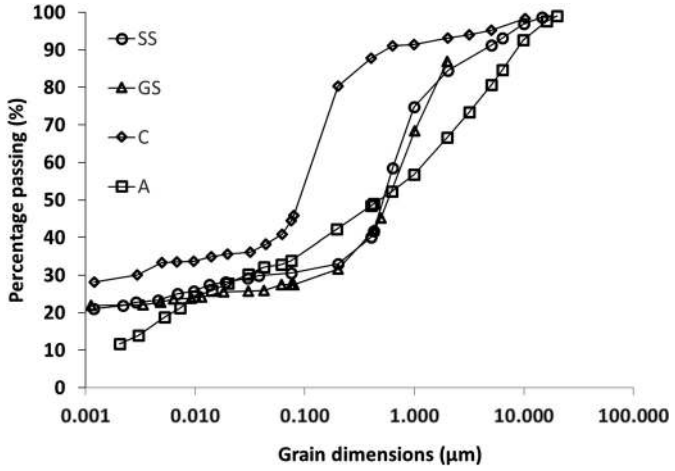

Fig. 1. Grain-size distribution of soils tested

Study of Evolution of Hydraulic Parameters

Hydraulic parameter corresponds to the infiltration flow-rate evolutions depending on the hydraulic gradient applied to the sample. By varying this parameter, it is possible to adapt the hydraulic stress to reach the maximum stress value of the sample, depending on its vertical position under the ground surface. Thus, the couple confining pressure/injection pressure allows the reproduction of the external stresses applied to the sample.

Four permeability test series were carried out on the compacted soils. The degrees of compaction are 85, 95, 100, and 105% of OPN, respectively. To ensure a better representativeness of the results, permeability tests were duplicated (two specimens tested for each targeted degree of compaction). This represents a total of 32 permeability tests with an average duration of 2 months. A microstructural characterization of tested samples was done after permeability test (the "Light Microscopic Observations" section). The samples tested were prepared by static compaction (using a hydraulic press that can support up to 50 kN) in cylindrical core barrels of 5-cm diameter and 10-cm height.

Experimental Setup for Permeability Tests

Permeability tests were carried out by using a flexible-wall permeameter (Fig. 3). The tested sample is sealed in a cellulose membrane. Then, it is placed into a rigid transparent PVC cell with a porous stone on its top and on its bottom. The PVC cell is equipped with a water inlet valve for the application of the confining pressure in between the cell and cellulose membrane.

Hydraulic Test Protocol

The confining pressure is applied at least 24 h prior to application of the injection pressure. The value of the confining pressure is 2 times higher than that of the injection pressure. This procedure is devoted to maintaining the structure of the compacted sample against

Table 3. Physical Properties of Soils Studied at OPN

Soil	Compaction mode	Water content at OPN (%)	Dry density (kN/m^3)
SS	Static	13.16	19.25
GS		12.89	19.55
C		19	17.53
A		13.14	19.45

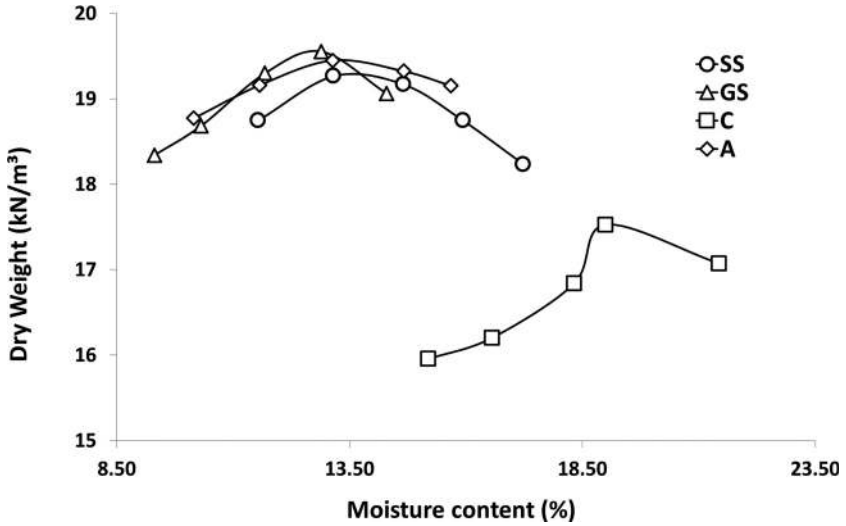

Fig. 2. Compaction curves of soils tested

microstructure change due to the hydraulic head. For permeability tests carried out in this study, the maximum hydraulic stress applied to the samples corresponds to an embankment of 4-m height (80 kPa). The water flow is measured once a steady-state regime is achieved. The percolating solutions are then collected to record the flow-rate evolutions and to measure the pH value and the electrical conductivity. Tests are stopped once the following criteria have been met: stabilization of the flow rates (condition of validity of Darcy's law), stabilization of the electrical conductivity, and linearity of Darcy's law. At the end of permeability tests, the geometrical and physical properties of the specimens are controlled.

Light Microscopic Observations

Light microscopic examinations of the tested samples were performed after permeability tests. To preserve the sample microstructure, drying processes were done by sublimation with the lyophilization method. Samples were then cut into cubes with approximately 25-mm sides, placed in a cylindrical mold of 25-mm diameter, and vacuum impregnated with an acrylic resin LR White hard grade. Such resin contains a fluorescent pigment known as Tinopal OB (approximately 1%; BASF, Florham Park, New Jersey), which allows the voids in the soil to be highlighted under a natural and/or polarized light source and hence estimates the bidimensional porosity (voids filled with pigmented resin). To improve the examination of the microstructure, the surface of the impregnated samples was polished by using a semiautomatic polisher (StruersTegra System Struers, Ballerup, Denmark). The light microscope used is an ECLIPSE LV100 (Nikon, Melville, New York) with a magnification from 2.5× up to 100× under white light or ultraviolet light on flat surfaces. Magnifications of 2.5× and 5× were adopted in this study. The image processing and acquisition were realized by using a charged-coupled device (CCD) Nikon DS-2Mv camera and software. This tool provides additional information about the compaction effects on the grain packing.

Fig. 3. Flexible-wall permeameters used for permeability tests

Results Obtained on Compacted Soils

MIP Tests Results

The pore-size distribution curves of tested soils are shown in Figs. 4–7. The porosity and mode values are reported in the Appendix. For the SS (Fig. 4), the pore-size distribution is trimodal. The first mode, observed at approximately 60 μm for a degree of compaction of 85% OPN, tends to shift to the right as the degree of compaction increases, concomitantly with a decrease in the overall porosity. The two other *pseudomodes* are localized at approximately 1.3 and 0.02 μm, respectively.

For the GS (Fig. 5), the pore-size distribution is bimodal. The first mode, appearing at approximately 30 μm for a degree of compaction of 85% OPN, tends to shift to the right as the degree of compaction increases, concomitantly with a decrease in the overall porosity as previously observed for SS. The second mode is localized at approximately 0.01 μm.

For the C (Fig. 6), the pore-size distribution is also bimodal. A reduction of the overall porosity is observed as the degree of compaction increases, in addition to a decrease in the first mode value, which is equal to 45 μm for a degree of compaction of 85%. The second

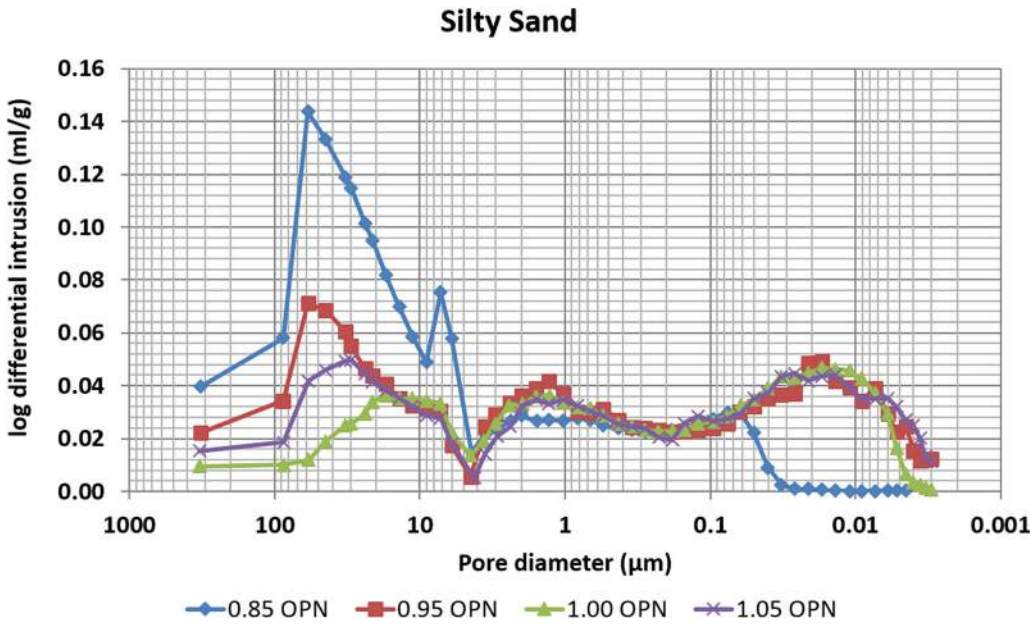

Fig. 4. Pore-size distributions of SS for degrees of compaction adopted in this study

mode is localized at approximately 0.01 μm. For A (Fig. 7), the pore-size distribution is unimodal, with a mode localized at approximately 1 µm for a degree of compaction of 85% OPN, and tends to shift slightly to the right as the degree of compaction increases without a significant reduction in the overall porosity due to the brittleness of the A as confirmed by the light microscopic examination results (the "Light microscopic Observation Results" section).

Water Permeability Results

The experimental permeability values obtained for the different degrees of compaction are shown in Table 4. Table 4 highlights a classification of the materials according to their mineralogical characteristics. Indeed, for a given degree of compaction, the permeability value is not the same from one material to another. It is worth noting that the permeability values shown here are consistent with those found in the literature. However, for the C and the two sands (SS and GS), a trend in decreasing permeability values of 2–3 orders of magnitude is observed as the degree of compaction increases. Beyond the reduction of the overall porosity and of the pore sizes, those permeability evolutions can be associated with a change in the pore network interconnection due to compaction effects. This is illustrated in Fig. 8, which shows a significant reduction of water-flow paths after compaction. For the A, the evolution of the permeability is less significant when the degree of compaction increases (only approximately 1 order of magnitude). This is probably due to the brittleness of the A, which leads to a disparity of permeability results.

Light Microscopic Observation Results

The light microscopic observation results are shown in Figs. 9–12. The dark background corresponds to the solid phase of the material, and the white motifs represent the voids inside the material. For the SS (Fig. 9), voids become narrower as the degree of compaction

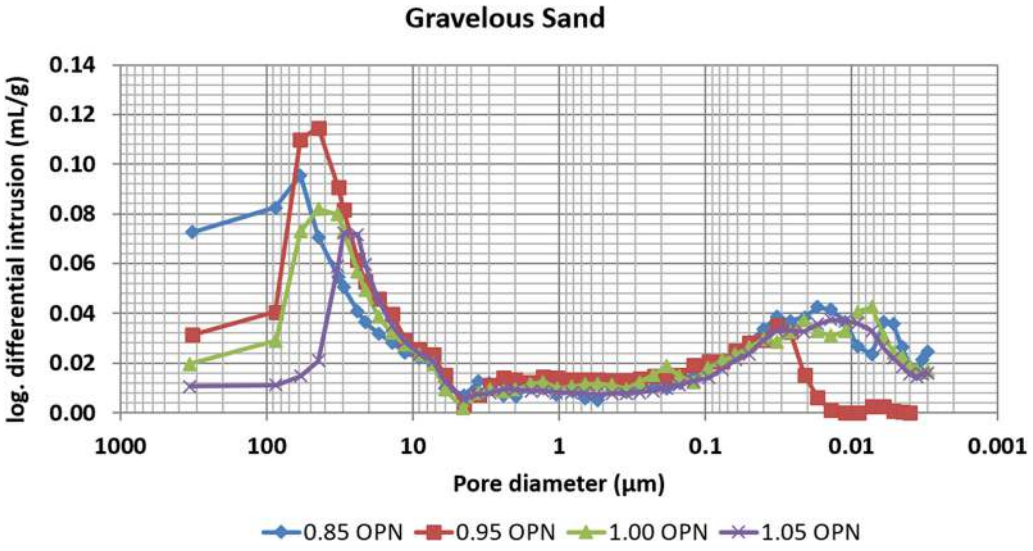

Fig. 5. Pore-size distributions of GS for degrees of compaction adopted in this study

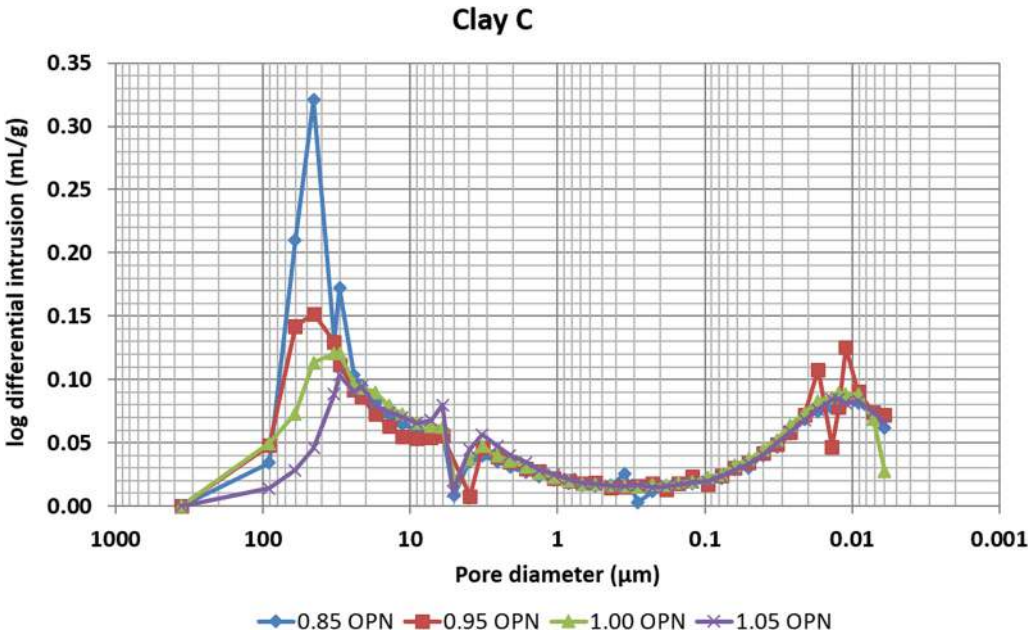

Fig. 6. Pore-size distributions of C for degrees of compaction adopted in this study

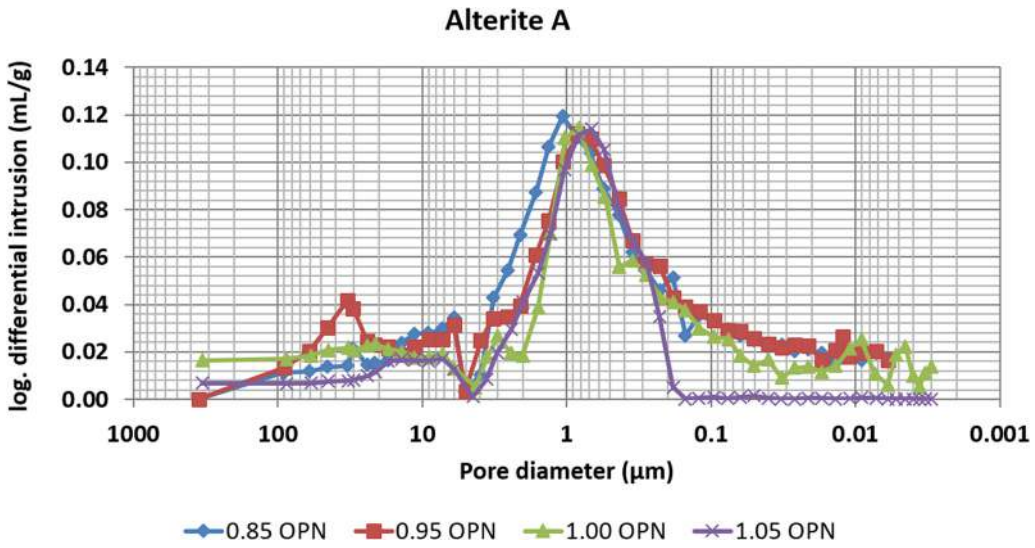

Fig. 7. Pore-size distribution of A for degrees of compaction adopted in this study

Table 4. Water Permeability Results

Sample	Degree of compaction (% of OPN)	Water permeability (10^{-15} m^2)
SS	85	5,500
	95	11.4
	100	1.14
	105	Not measured
GS	85	93,900
	95	1,510
	100	8.75
	105	1.52
C	85	6,650
	95	63
	100	1.21
	105	2.05
A	85	36.7
	95	31.1
	100	9.82
	105	6.89

increases due to the filling of voids not occupied by sand grains with finer particles. The increase in grain cohesion is therefore improved by the compaction. These observations are consistent with MIP test results shown in Fig. 4. As observed for the SS, the interaggregate voids also become narrower as the degree of compaction increases for the GS (Fig. 10). This is of course due to the mineralogy of the tested materials. For the C (Fig. 11), a narrowing of voids with an increase of the degree of compaction is also highlighted. Such a result is consistent with the MIP test results shown in Fig. 6. The A exhibits a relatively dense structure compared to the other soils (Fig. 12). The effects of compaction are observed visually but remain very limited. Indeed, A has a layered structure, which may be destructured by the compaction process.

Proposition of a New Predictive Model of Permeability of Compacted Soils: Validation of Soil Permeability Models Involving Microstructural Properties on Soils Tested in the Study

This section is dedicated to the proposition of a new soil permeability model involving microstructural properties and compaction characteristics. First, four models among all approaches discussed in the "State of the Art" section were selected—Carman-Kozeny model [Eq. (4)], Aït-Mokhtar et al. (1999) model [Eq. (6)], Amiri et al. (2005) model [Eq. (7)], and Katz and Thompson (1986) model [Eq. (8)], respectively—to confirm the necessity of considering compaction characteristics in the prediction of soil permeability. The four models tested here are based only on microstructural characteristics. Second, the authors will determine how to associate the compaction characteristics with the microstructural properties to obtain a well-defined model from a physical and geotechnical point of view. The permeability values estimated from the four previously selected models are given in Table 5. According to the values shown in Table 5, the permeability values provided by the model developed by Amiri et al. (2005) and by the Carman-Kozeny approach are largely underestimated compared to experimental values. In fact, the model proposed by Amiri et al. (2005), which is a serial pore model, was especially developed for cement-based materials. The main parameter involved in the model is the smallest pore size belonging to a percolation path [Eq. (7)] rather than larger pores, which govern the permeability of soils. The influence of the macroporosity is taken into account in the model through morphological parameters, which are estimated from empirical considerations. The low permeability values calculated with the Carman-Kozeny approach can be explained by an imprecise estimation of specific surface area by MIP tests, as well as by the possibility that the model is not valid for some types of soil, even if this hypothesis has been questioned by some authors ("State of the Art").

The model developed by Aït-Mokhtar et al. (1999) and the Katz-Thompson approach rather overestimate permeability values. This is quite normal because, in these approaches, the permeability is mainly governed by large pores associated with the macroporosity. It is interesting to note that, for a degree of compaction of 85% OPN, the two models provide values of permeability close to those obtained experimentally. However, a difference of 2–3 orders of magnitude is observed between the calculated permeabilities and those measured as the degree of compaction increases. These results highlight that the sole consideration of the pore size evolutions is not enough to achieve a relevant prediction of soil permeability. Indeed, in addition to modifying the porosity and the pore-size distribution, the compaction characteristics also affect the interconnection of the porous structure. Consideration of these aspects in the modeling of soil permeability is

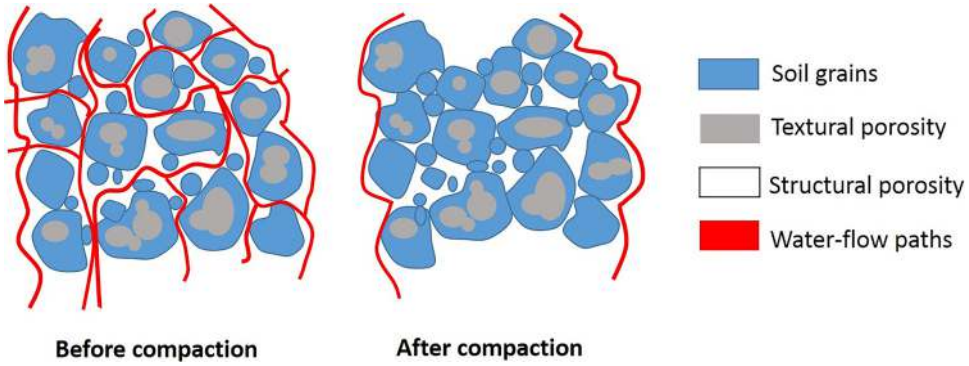

Fig. 8. Evolution of water-flow paths with compaction

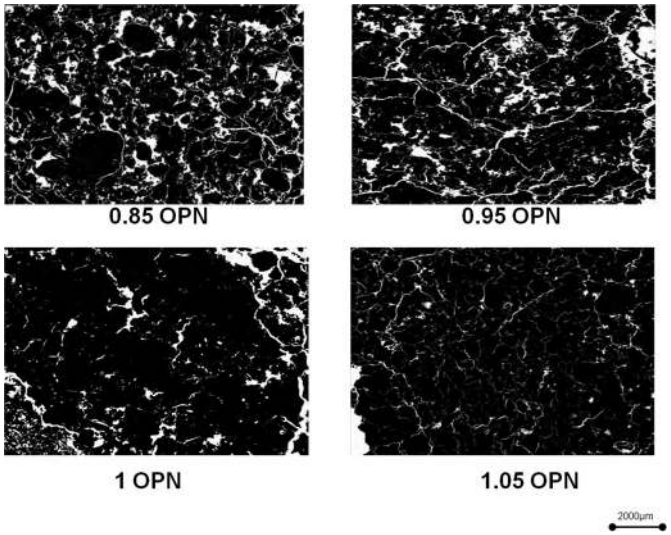

Fig. 9. Mapping of SS with light microscopy

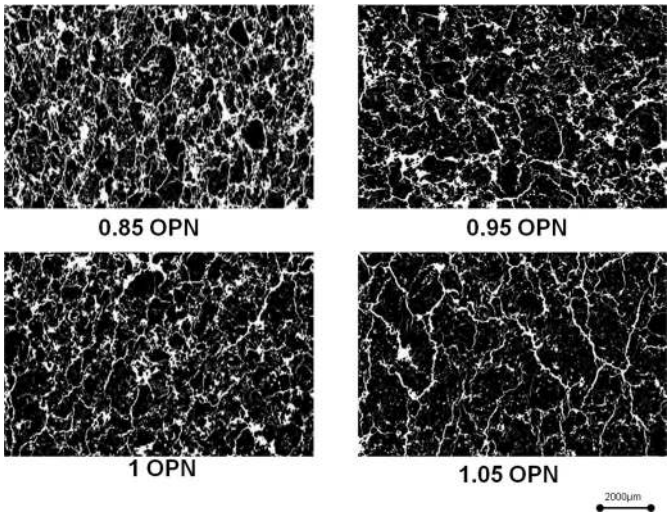

Fig. 11. Mapping of C with light microscopy

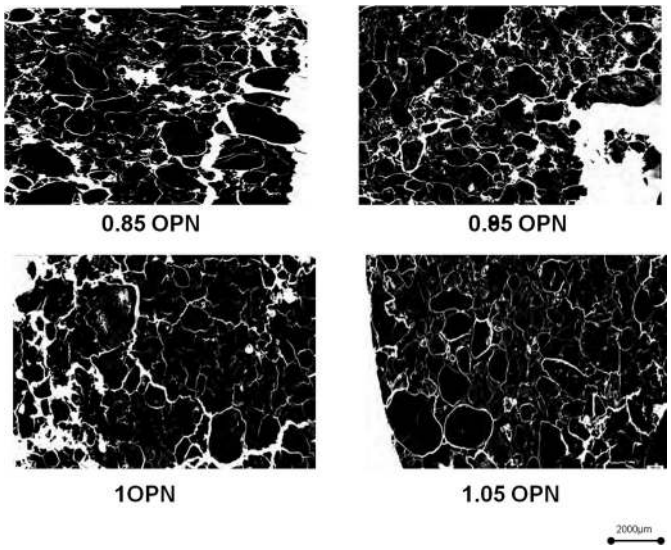

Fig. 10. Mapping of GS with light microscopy

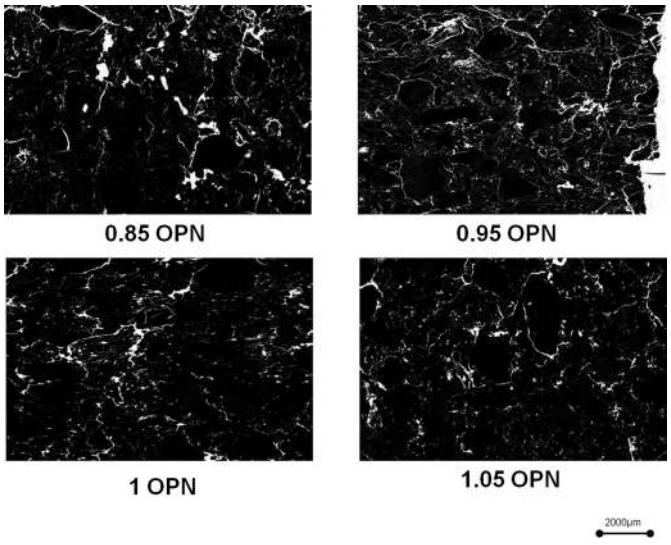

Fig. 12. Mapping of A with light microscopy

discussed in the next section. However, it is important to note that the case of A is different from that of the other soils. Indeed, regardless of the degree of compaction, the model developed by Aït-Mokhtar et al. (1999) and the Katz-Thompson approach allow the reproduction of the experimental values. In this case, the impact of the compaction characteristics on the morphological parameters of the porous

Table 5. Comparison between Experimental Permeability Values and Those Provided by Permeability Soil Models Involving Microstructural Properties

Samples	Degree of compaction (%)	Katz and Thompson (1986) (10^{-16} m^2)	Carman-Kozeny (10^{-19} m^2)	Aït-Mokhtar et al. (1999) (10^{-15} m^2)	Amiri et al. (2005) (10^{-22} m^2)	Experimental results (10^{-15} m^2)
SS	85	168,000	2,690	23,300	204,000,000	5,500
	95	275,000	74.6	25,400	2,120,000	11.4
	100	86,700	17.3	4,560	2,980,000	1.14
GS	85	66,200	54.5	39,200	4.73	93,900
	95	97,800	110	12,500	20.9	1,510
	100	97,100	11.8	13,600	0.352	8.75
	105	31,700	1.19	1,950	2.46	1.52
C	85	263,000	4,440	29,000	3.77	6,650
	95	333,000	5,210	32,200	4.03	63
	100	138,000	93.2	10,000	2.39	1.21
	105	193,000	27.9	5,720	45,000,000	2.05
A	85	2,530	204	24.3	12,900,000	36.7
	95	1,760	215	3,480	439,000	31.1
	100	8.45	143	14.1	9,200,000	9.82
	105	12.2	396	3.58	2,300,000	6.89

Table 6. Comparison between Experimental Permeability Values and Those Provided by Modified Version of Model Developed by Aït-Mokhtar et al. (1999)

Samples	Degree of compaction (%)	Exponent m value	Aït-Mokhtar et al. (1999) modified model (10^{-16} m^2)	Experimental results (10^{-15} m^2)
SS	85	45.29	77,800	5,500
	95		13,000	11.4
	100		980	1.14
GS	85	5.33	130,000	93,900
	95		23,000	1,510
	100		19,000	8.75
	105		2,110	1.52
C	85	45.29	96,900	6,650
	95		630	63
	100		18.5	1.21
	105		1.10	2.05

structure is probably limited due to the brittleness of the A, whose microstructure is destructurated under the effect of compaction.

Consideration of Compaction Characteristics in Prediction of Permeability of Compacted Soils

As seen in the previous section, the model developed by Aït-Mokhtar et al. (1999) and the Katz-Thompson approach can be used to predict the permeability of compacted soil, providing that the impact of compaction characteristics on the interconnection of the porous structure are also taken into account. In this paper, the authors opt for using the model proposed by Aït-Mokhtar et al. (1999) because the Katz-Thompson approach involves an empirical coefficient whose value can vary from one material to another (cf. literature review). Moreover, the formation resistivity factor (σ/σ_0) has been estimated from MIP test results, according to the calculation method proposed by Katz and Thompson (1986). However, the complexity of the chemical equilibria between liquid and solid phases requires the use of a more relevant method to calculate this parameter. For this reason, the model proposed by Aït-Mokhtar et al. (1999) is more relevant. As mentioned previously, the soil permeability decreases as the degree of compaction increases not only because of the evolution of the porosity and the pore-size distribution, but also because of the evolution of pore interconnections. To consider the compaction effect, the model developed by Aït-Mokhtar is thus modified as follows:

$$k = C(f) \sum_{j=1}^{N} e 6 \xi_j^2 \frac{\varepsilon_{pjr_{pmj}^2}}{24} \tag{10}$$

where $C(f)$ = interconnection function of pores, which depends on the degree of compaction, noted as f. In this version of the model, the authors assume that permeability is isotropic, unlike the original version of the model [Eq. (6)].

The interconnection function (C) is given by the following relationship:

$$C(f) = \begin{cases} 1 \text{ if } f \leq 85\% \text{ OPN} \\ \left(\dfrac{0,85}{f}\right)^m \text{ if } f > 85\% \text{ OPN} \end{cases} \tag{11}$$

As reported in the previous paragraph, the experimental values of permeability are well-reproduced by the model proposed by Aït-Mokhtar et al. (1999) for a degree of compaction of 85% OPN. For this reason, it is considered that, for a degree of compaction lower than 85% OPN, the connectivity value is equal to 1 because the soil density is lower so that the porosity is more interconnected. However, this connectivity value gradually decreases with a nonlinear evolution as the degree of compaction increases, because a reduction of the experimental permeability values by 2–3 orders of magnitude was observed. This is the reason why the connectivity function was expressed by using a power function with an exponent noted as m. This nonlinearity can be associated with the granulometric characteristics of the soil. In fact, those granulometric characteristics necessarily play a role in the evolution of the pore interconnections by blocking the water-flow paths and by modifying the morphological parameters (Fig. 8). Indeed, the optimum Proctor can be assimilated in a simplified way to a granular packing with the lowest porosity. Such a process necessarily involves both grain shapes and sizes. For the exponent m, the authors consider the two most-used parameters characterizing the grain-size distribution: the curvature coefficient (C_c) and the uniformity coefficient (C_u)

$$C_c = \frac{d_{30}^2}{d_{60} \times d_{10}} \tag{12}$$

$$C_u = \frac{d_{60}}{d_{10}} \tag{13}$$

where d_i = diameter of the sieve corresponding to a percentage passing of i%.

By combining Eqs. (12) and (13)

$$\frac{C_u}{C_c} = \left(\frac{d_{60}}{d_{30}}\right)^2 \tag{14}$$

As a first approach, the authors propose for the exponent m

$$m = \sqrt{\frac{C_u}{C_c}} = \frac{d_{60}}{d_{30}} \tag{15}$$

Finally

$$C(f) = \begin{cases} 1 \text{ if } f \leq 85\% \text{ OPN} \\ \left(\dfrac{0,85}{f}\right)\dfrac{d_{60}}{d_{30}} \text{ if } f > 85\% \text{ OPN} \end{cases} \tag{16}$$

A comparison of permeability values calculated from the modified version of the model developed by Aït-Mokhtar et al. (1999) and those obtained experimentally is presented in Table 6. The new approach proposed for predicting the permeability of compacted soils reproduces the experimental results in a satisfactory way, except those corresponding to the GS for degrees of compaction of 100 and 105% OPN and those corresponding to SS for the degrees of compaction of 100 and 95%. This can be explained by the fact that the influence of the compaction characteristics is probably more or less significant than that provided by the interconnection function proposed in this paper [Eq. (16)].

Conclusions

A new analytical model is proposed to predict the permeability of compacted soils. The model involves microstructural properties (porosity and pore-size distribution) and compaction characteristics that modify the interconnection of pores. The model is inspired from that developed by Aït-Mokhtar et al. (1999), representing the porous structure with parallel cylindrical channels that have been oriented in the three space directions. The influence of the compaction characteristics is considered in the model by introducing an interconnection function of pores. Such function is expressed by an inverse power law due to the nonlinear evolution of permeability values. The exponent involved in the power law is associated with granulometric characteristics of soils, which necessarily plays a role in the evolution of the pore interconnections, reduction of the water-flow paths, and modification of the morphological parameters of the porous structure. The model was tested on different soils: SS, GS, C, and A compacted at 85, 95, 100, and 105% of OPN, respectively. The experimental results of permeability fit well with the model, except for A. Indeed, due to the brittleness of the A, the compaction process leads to a destructuration of the material rather than to its densification, as confirmed by light microscopic observation and MIP test results. The extension of the model to the case of soils treated with hydraulic binders is one perspective of this study.

Appendix. MIP

Table 7 includes the MIP test results.

Table 7. MIP Test Results

Samples	Degree of compaction (%)	Materials data		First porous mode				Second porous mode				Third porous mode				
		$V\text{cum}_{,\text{total}}$ (mL/g)	Total porosity	$V\text{cum}_{,1}$ (mL/g)	Porosity	$d\text{max}_{,1}$ (μm)	$rp\text{max}_{,1}$ (μm)	$dV/d\log$ ($rp\text{max}_{,1}$)	$V\text{cum}_{,2}$ (mL/g)	Porosity	$d\text{max}_{,2}$ (μm)	$rp\text{max}_{,2}$ (μm)	$dV/d\log$ ($rp\text{max}_{,2}$)	$V\text{cum}_{,3}$ (mL/g)	Porosity	$d\text{max}_{,3}$ (μm)	$rp\text{max}_{,3}$ (μm)	$dV/d\log$ ($rp\text{max}_{,3}$)
SS	85	0.188	0.309	0.118	0.194	58.830	29.415	0.144	0.136	0.030	7.230	3.615	0.075	0.188	0.085	0.062	0.031	0.030
	95	0.166	0.430	0.068	0.176	58.830	29.415	0.071	0.108	0.103	1.294	0.647	0.042	0.166	0.151	0.017	0.009	0.049
	100	0.150	0.356	0.050	0.119	29.770	14.885	0.050	0.088	0.090	1.279	0.639	0.033	0.150	0.146	0.021	0.011	0.042
SG	85	0.162	0.415	0.100	0.256	58.800	29.400	0.095	0.162	0.159	0.017	0.009	0.043					
	95	0.133	0.248	0.090	0.168	44.300	22.150	0.115	0.133	0.080	0.032	0.016	0.035					
	100	0.132	0.331	0.070	0.176	44.280	22.140	0.082	0.132	0.155	0.007	0.004	0.043					
	105	0.103	0.213	0.046	0.095	23.940	11.970	0.072	0.103	0.118	0.014	0.007	0.038					
C	85	0.280	0.660	0.175	0.413	45.300	22.650	0.321	0.280	0.248	0.011	0.006	0.082					
	95	0.252	0.691	0.140	0.383	45.290	22.645	0.152	0.252	0.307	0.011	0.006	0.126					
	100	0.247	0.408	0.140	0.231	30.190	15.095	0.121	0.247	0.177	0.011	0.006	0.088					
	105	0.205	0.358	0.090	0.157	30.186	15.093	0.103	0.125	0.061	3.240	1.620	0.057	0.205	0.139	0.011	0.006	0.082
A	85	0.169	0.363	0.169	0.364	1.063	0.531	0.119										
	95	0.173	0.371	0.036	0.077	32.947	16.474	0.038	0.173	0.294	0.679	0.340	0.110					
	100	0.144	0.410	0.144	0.410	0.820	0.410	0.115										
	105	0.102	0.197	0.102	0.197	0.671	0.336	0.114										

References

Ahangar-Asr, A., Faramarzi, A., Mottaghifard, N., and Javadi, A. A. (2011). "Modeling of permeability and compaction characteristics of soils using evolutionary polynomial regression." *Comput. Geosci.*, 37(11), 1860–1869.

Aït-Mokhtar, A., Amiri, O., and Sammartino, S. (1999). "Analytic modelling and experimental study of the porosity and permeability of a porous medium-application to cement mortars and granitic rock." *Mag. Concr. Res.*, 51(6), 391–396.

Aldeef, A. A., and Rayhani, M. T. (2014). "Hydraulic performance of compacted clay liners (CCLs) under combined temperature and leachate exposures." Waste Manage., 34(12), 2548–2560. 10.1016/j.wasman .2014.08.007.

Amiri, O., Aït-Mokhtar, A., and Sarhani, M. (2005). "Tri-dimensional modelling of cementitious materials permeability from polymodal pore size distribution obtained by mercury intrusion porosimetry tests." *Adv. Cem. Res.*, 17(1), 39–45.

Banavar, J., and Johnson, D. L. (1987). "Characteristic pore sizes and transport in porous media." *Phys. Rev. B: Condens. Matter*, 35(13), 7283–7286, 9941024.

Beven, K., and Germann, P. (1982). "Macropores and water flow in soils." *Water Resour. Res.*, 18(5), 1311–1325.

Chapuis, R. P. (2004). "Predicting the saturated hydraulic conductivity of sand and gravel using effective diameter and void ratio." *Can. Geotech. J.*, 41(5), 787–795.

Chapuis, R. P., and Aubertin, M. (2003). "On the use of the Kozeny-Carman equation to predict the hydraulic conductivity of soils." *Can. Geotech. J.*, 40(3), 616–628.

Childs, E. C., and Collis-George, N. (1950). "The permeability of porous materials." *Proc. Royal Soc. A*, 201(1066), 392–405.

Garcia-Bengochea, I. (1978). "The relation between permeability and pore size distribution of compacted clayey silts." MSCE thesis and Joint Highway Research Project Rep. No. 78-4, Purdue Univ., West Lafayette, IN.

Hazen, A. (1892). "Some physical properties of sand and gravel, with special reference to their use in filtration." *Publication No. 34*, 539–556, Massachusetts State Board of Health, Boston.

Juang, C. H., and Holtz, R. D. (1986). "A probabilistic permeability model and the pore density function." *Int. J. Numer. Anal. Methods Geomech.*, 10(5), 543–553.

Katz, A. J., and Thompson, A. H. (1986). "Quantitative prediction of permeability in porous rock." *Phys. Rev. B*, 34(11), 8179–8181, 9939522.

Kenney, T. C., Lau, D., and Ofoegbu, G. I. (1984). "Permeability of compacted granular material." *Can. Geotech. J.*, 21(4), 726–729.

Lambe, T. W., and Whitman, R. V. (1969). *Soils mechanics*, Wiley, New York.

Lapierre, C., Leroueil, S., and Locat, J. (1990). "Mercury intrusion and permeability of Louiseville clay." *Can. Geotech. J.*, 27(6), 761–773.

Le Doussal, P. (1989). "Permeability versus conductivity for porous media with wide distribution of pore sizes." *Phys. Rev. B*, 39(7), 4816–4819.

Saffman, P. G. (1959). "A theory of dispersion in a porous medium." *J. Fluid Mech.*, 6(3), 321–349.

Shackelford, C. D., Benson, C. H., Katsumi, T., Edil, T. E., and Lin, L. (2000). "Evaluating the hydraulic conductivity of GCLs permeated with non-standard liquids." *Geotext. Geomembr.*, 18(2–4), 133–161.

Slichter, C. S. (1898). "Theoretical investigation of the motion of ground waters." *U.S. Geological Survey 19th Annual Rep., Part II*, 295–384.

Taylor, D. W. (1948). *Fundamentals of soil mechanics*, John Wiley & Sons, New York.

Wang, M. C., and Huang, C. C. (1984). "Soil compaction and permeability prediction model." *J. Environ. Eng.*, 10.1061/(ASCE)0733-9372(1984)110: 6(1063), 1063–1083.